Theor Chem Account (2009) 122:275–281
DOI 10.1007/s00214-009-0506-3

REGULAR ARTICLE

Fluorinated derivatives of *mer*-Alq3: energy decomposition analysis, optical properties, and charge transfer study

Ahmad Irfan · Ruihai Cui · Jingping Zhang

Received: 5 November 2008 / Accepted: 5 January 2009 / Published online: 18 January 2009
© Springer-Verlag 2009

Abstract Equilibrium geometry configurations of the mono-fluorinated derivatives of the meridianal isomer of tris(8-hydroxyquinolinato)aluminum (*mer*-Alq3) are calculated at the B3LYP/6-31G* level. The lowest singlet excited states (S_1) have been optimized by the singles configuration interaction (CIS/6-31G*) approach. The absorption and emission spectra were evaluated at the TD-PBE0/6-31G* level. A significant blue shift was predicted for tris(4-fluoro-8-hydroxyquinolinato)aluminum derivative (4FAlq3) while a significant red shift was observed for tris(5-fluoro-8-hydroxyquinolinato)aluminum (5FAlq3). Energy decomposition analysis has been performed at the B3LYP/DZP level. On the basis of energy decomposition analysis, we have explained the distribution pattern for frontier molecular orbitals. We have found that no contribution of improvement for intrinsic charge mobility for the mono-fluorine substituted *mer*-Alq3.

Keywords *mer*-Alq3 · Energy decomposition analysis · Optical properties · Reorganization energy

Electronic supplementary material The online version of this article (doi:10.1007/s00214-009-0506-3) contains supplementary material, which is available to authorized users.

A. Irfan · J. Zhang (✉)
Faculty of Chemistry, Northeast Normal University,
130024 Changchun, China
e-mail: zhangjingping66@yahoo.com.cn

R. Cui
Department of Chemistry, Harbin University,
150080 Harbin, China

1 Introduction

Organic light-emitting diodes (OLEDs) have rapidly developed over the last decade and have become the highly competitive alternative of full color flat panel display [1–4]. The OLEDs are heterojunction devices in which layers of organic transport materials are usually incorporated into devices as amorphous thin solid films [5]. The *mer*-Alq3 has been a key compound for organic electroluminescence (EL) devices [6–12] since the first realization of a multi-layered EL device by Tang and Van Slyke [13]. The electronic structures of *mer*-Alq3-like complexes can be tuned by adding substituents to quinolate ligand. In general, electron donating groups (EDGs) attached to pyridine ring causes a blue shift in complex emission [14–16] while introduction to phenoxide ring causes a red shift [15, 16]. The tris(5-*x*-8-quinolinolato)aluminum and tris(7-*x*-8-quinolinolato)aluminum (*x* is electron-withdrawing group (EWG) such as chloro- [17] and cyano [18]) show almost negligible emission shifts, while strong EWGs such as sulfonamide ($-SO_2NR2$) result in significantly blue-shifted emission [19]. The introduction of fluorine into organic compounds can profoundly influence their chemical and physical properties when compared to their non-fluorine containing analogs, leading to a range of man-made materials with highly desirable properties [20].

Shi et al. [21] experimentally synthesized fluorinated derivatives of *mer*-Alq3, i.e., tris(*n*-fluoro-8-hydroxyquinolinato)aluminum (nFAlq3, $n = 5, 6, 7$). The present work is in detailed theoretical study on the fluorinated derivatives of *mer*-Alq3, i.e., energy decomposition analysis, optical properties, and reorganization energy. We designed two new derivatives, i.e., tris(3-fluoro-8-hydroxyquinolinato)aluminum (3FAlq3) and tris(4-fluoro-8-hydroxyquinolinato)aluminum (4FAlq3).

In the framework of Kohn–Sham Molecular Orbital theory and in conjunction with the fragment approach, one can decompose the bond energy between the fragments of a molecular system into contributions associated with the various orbital and electrostatic interactions, method known as energy decomposition analysis (EDA) [22]. Energy decomposition analysis of the bonding between the fragments AlL_2^+ (Al along with any two ligands among ligand-A, ligand-B, and ligand-C) and a single ligand L_i^- (L_i = A, B or C ligand) have been performed, with the aim to rationalize the distribution pattern of HOMOs and LUMOs. The over all bond energy ΔE is divided into two major components (Eq. 1): the preparation energy ΔE_{prep} corresponding to the amount of energy required to deform the separated fragments, from their equilibrium structure to the geometry they acquire in the overall molecule ($\Delta E_{prep,geo}$), and to excite them to their valence electronic configuration ($\Delta E_{prep,el}$). In the second term, the interaction energy ΔE_{int} between the prepared fragments.

$$\Delta E = \Delta E_{prep} + \Delta E_{int} = \Delta E_{prep,geo} + \Delta E_{prep,el} + \Delta E_{int} \quad (1)$$

The interaction energy ΔE_{int} is further decomposed into three physically meaningful terms.

$$\Delta E_{int} = \Delta E_{elst} + \Delta E_{pauli} + \Delta E_{oi} \quad (2)$$

The term ΔE_{elst} is associated with the electrostatic interaction between the unperturbed charge distributions of the prepared fragments as they are brought together at their final positions, yielding the overall density that is simply a superposition of fragment densities $\rho_A + \rho_B$. The repulsive term ΔE_{pauli} is caused by going from the product of fragment wave functions ψ_A and ψ_B to $\psi^0 = NA[\psi_A\psi_B]$ that properly obeys the Pauli principle (A antisymmetrization operator, N renormalization constant). The orbital interaction energy ΔE_{oi} is the energy change due to the relaxation of the wave function to its final form through electron pair bonding, charge transfer and polarization. The orbital term ΔE_{oi} can be considered as an estimate of the covalent contributions to the attractive interactions. Thus, the ratio $\Delta E_{elst}/\Delta E_{oi}$ indicates the electrostatic/covalent character of the bond. Details can be found in [22].

The bonding interactions have been analyzed by means of EDA [23–26] developed by Ziegler and Rauk [27] for DFT methods and incorporated in ADF [26]. The EDA method is related to the energy partitioning scheme of *Morokuma* which was introduced earlier for Hartree–Fock calculations [28]. The advantage of DFT compared with HF calculations is that the Kohn–Sham orbitals include correlation effects while HF orbitals do not [22].

2 Computational details

The calculations described here were carried out using the Gaussian 03 suite of program [29]. The structures of different mono-fluorinated derivatives of *mer*-Alq3 were optimized in the ground states (S_0) at the B3LYP/6-31G* level, which has been proved to be an efficient approach for *mer*-Alq3 and it derivatives [30–33]. The low lying excited state structure (S_1) was optimized using the configuration interaction with single excitations (CIS) approach by Hall and Schlegel [34]. In our group the same approach has been applied on *mer*-Alq3 [30, 31] and its nitrogen derivatives [32] as well as other OLED materials [35–38], which gave accurate and reliable results. So in this study to optimize the geometry of the S_1, CIS was used with 6-31G* basis set. The absorption and emission spectra were calculated by time dependent density functional theory (TD-DFT) using PBE0 [39] with the 6-31G* [40] basis set. The reorganization energy that is one of the important parameters of mobility has been calculated at the B3LYP/6-31G* level of theory.

The calculations for energy decomposition analysis were carried out with the program package ADF [41]. We performed energy decomposition analysis of the chemical bonds at the B3LYP/DZP level [33]. Scalar relativistic effects were considered by using the zero-order regular approximation (ZORA) [42] on optimized structures at the B3LYP/6-31G* level.

3 Results and discussion

3.1 Molecular geometries at the ground states

Figure 1a is labeled with A–C designating the three different quinolate ligands of *mer*-Alq3. The structure is such that the central Al atom (+3 formal oxidation state) is surrounded by the three quinolate ligands in a pseudo-octahedral configuration with the A- and C-quinolate nitrogens and the B- and C-quinolate oxygens trans to each other. The molecular models used in our calculations, obtained by systematic substitution of fluorine atom in positions 3, 4, … 7 (see labeling scheme) on each ligand are shown in Fig. 1b. Table 1 presents the optimized and available experimental [43] values of bond lengths and bond angles obtained for the *mer*-Alq3 and its fluorinated derivatives. Comparative to optimized *mer*-Alq3, the Al–N bonds are predicted to be negligible lengthened in 3FAlq3 (0.009 Å) and 5FAlq3 (0.009 Å) while negligible shortened in 4FAlq3 (0.004 Å) and 6FAlq3 (0.004 Å). The Al–O bonds are also predicted to be generally negligible lengthened in 4FAlq3 and 6FAlq3, i.e., 0.002 Å while shortened in 3FAlq3 and 5FAlq3 within 0.006 and

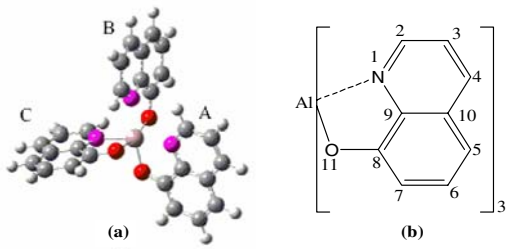

n	Different ligands	Complexes
3	tris(3-fluoro-8- hydroxyquino-linato) Aluminum	3FAlq3
4	tris(4-fluoro-8- hydroxyquino-linato) Aluminum	4FAlq3
5	tris(5-fluoro-8- hydroxyquino-linato) Aluminum	5FAlq3
6	tris(6-fluoro-8- hydroxyquino-linato) Aluminum	6FAlq3
7	tris(7-fluoro-8- hydroxyquino-linato) Aluminum	7FAlq3

n = 3, 4,.., 7 substituted "H" position by mono-fluorine atom as labeled in Fig. 1(b)

Fig. 1 **a** The geometry of *mer*-Alq3 with labels *A*–*C* for three quinolate ligands **b** the ligand labeling for substituted *mer*-Alq3 complexes considered in this work

0.003 Å, respectively. The bond lengths of Al–N and Al–O of 7FAlq3 are almost similar as in *mer*-Alq3.

3.2 Electronic structure

In the ground states HOMOs are localized mostly on A-ligand while LUMOs are localized on B-ligand in *mer*--Alq3 [30] and its nitrogen derivatives [33]. The HOMOs and LUMOs distribution pattern of fluorinated derivatives of *mer*-Alq3 in the S_0 states have been shown in the supporting information (Fig. S1) suggesting the localization of molecular orbitals. The HOMOs and LUMOs in the fluorinated derivatives of *mer*-Alq3 show the similar trend of localization at A and B ligands, respectively. As shown in Fig. 2 (for 3FAlq3 and 4FAlq3) and Fig. S2 (for 5FAlq3, 6FAlq3 and 7FAlq3) that LUMOs+1 are mostly localized on C-ligand and on the N, C1 and C3 (pyridyl ring) of A-ligand. The HOMO energy of 5FAlq3 is the highest among all the fluorinated derivatives due to the participation of F in the formation of HOMO (see HOMO of Fig. S2) which is in good agreement with experimental results [21]. In 4FAlq3 the F group in C-4 position takes part in the formation of LUMO and LUMO+1 (see Figs. 2, S1), thus giving rise to the higher LUMO and LUMO+1 energy levels. From Table 2, it can be found that the energy levels of the HOMO, LUMO and LUMO+1 of *mer*-Alq3 are higher than that of its fluorinated derivatives. Among different fluorinated derivatives, the trends of HOMOs, LUMOs, and LUMOs+1 energies are in the sequence of 5FAlq3 > 7FAlq3 > 4FAlq3 > 3FAlq3 > 6FAlq3, 4FAlq3 > 7FAlq3 > 6FAlq3 ∼ 5FAlq3 > 3FAlq3, and 4FAlq3 > 7FAlq3 > 6FAlq3 ∼ 5FAlq3 > 3FAlq3, respectively. The energy levels of the LUMO and LUMO+1 of 4FAlq3 are higher than that of other derivatives because F is taking part in the formation of LUMO and LUMO+1. The trend of gap energies is in the sequence of 4FAlq3 > 6FAlq3 > *mer*-Alq3 > 7FAlq3 ∼ 3FAlq3 > 5FAlq3. There is negligible difference between the gap energies of 7FAlq3 and parent molecule (*mer*-Alq3).

In the first excited states, as shown in Fig. 3 (for 3FAlq3 and 4FAlq3) and Fig. S3 (for 5FAlq3, 6FAlq3 and 7FAlq3), HOMOs are located on the phenoxide ring of A-ligand, while LUMOs are located on the pyridyl ring of A-ligand. From Fig. S3, it can be found that the F of 5FAlq3 is taking part in the formation of HOMO, raising the HOMO energy. In 4FAlq3 the F group in C-4 position takes part in the formation of LUMO (see LUMO Fig. 3), giving rise to the higher LUMO energy level of the 4FAlq3. In Table 3, the tendency of HOMOs and LUMOs energies among fluorinated derivatives are in the sequence of 5FAlq3 > 7FAlq3 > 4FAlq3 > 3FAlq3 > 6FAlq3 and 4FAlq3 > 7FAlq3 > 6FAlq3 ∼ 5FAlq3 > 3FAlq3, respectively. The trend of gap energies is in the sequence of 4FAlq3 > 6FAlq3 > *mer*-Alq3 > 7FAlq3 ∼ 3FAlq3 > 5FAlq3.

Table 1 Selected optimized bond lengths in angstrom (Å) and bond angles (°) for *mer*-Alq3 and its mono-fluorinated derivatives at the B3LYP/6-31G* level

Parameters	Alq3	3FAlq3	4FAlq3	5FAlq3	6FAlq3	7FAlq3	Exp[a]
Bond lengths							
$Al–N_A$	2.084	2.088	2.083	2.088	2.082	2.085	2.050
$Al–N_B$	2.126	2.135	2.122	2.135	2.122	2.128	2.087
$Al–N_C$	2.064	2.068	2.061	2.068	2.062	2.062	2.017
$Al–O_A$	1.855	1.852	1.856	1.852	1.857	1.855	1.850
$Al–O_B$	1.881	1.875	1.882	1.878	1.882	1.882	1.860
$Al–O_C$	1.884	1.879	1.886	1.882	1.885	1.885	1.857
Bond angles							
$N_A–Al–N_C$	171.5	171.3	171.4	171.5	171.3	171.2	173.8
$N_B–Al–O_A$	172.6	172.5	172.6	172.8	172.6	172.7	171.5
$O_C–Al–O_B$	166.6	166.0	166.6	166.2	166.9	166.1	168.2

[a] Experimental data of *mer*-Alq3 from [43]

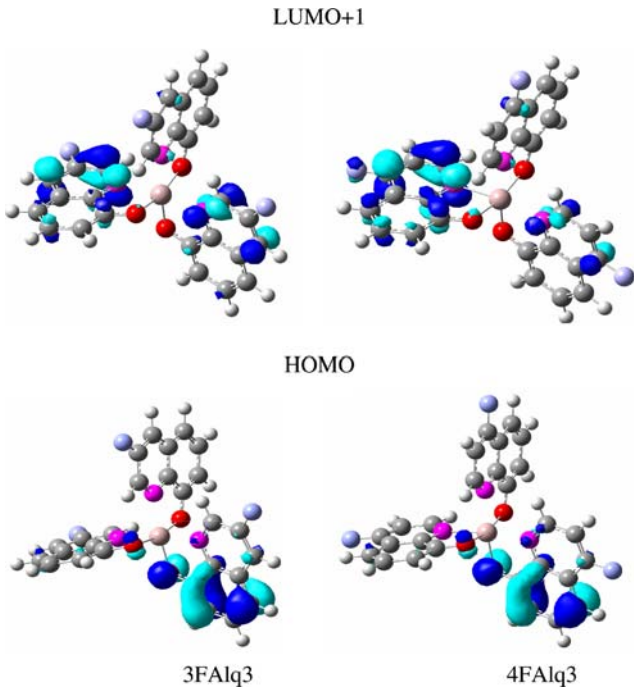

Fig. 2 Frontier molecular orbitals (FMOs) (0.05 e au^{-3}) for the ground state (S_0) of fluorinated substituted derivatives on position 3 and 4 of *mer*-Alq3

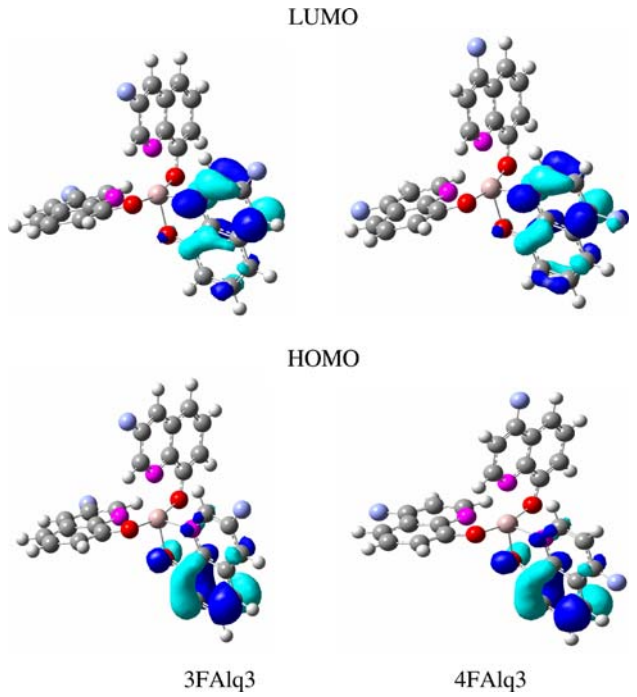

Fig. 3 Frontier molecular orbitals (FMOs) (0.05 e au^{-3}) for the excited state (S_1) of fluorinated substituted derivatives on position 3 and 4 of *mer*-Alq3

Table 2 The HOMO, LUMO, LUMO+1, and gap energies (E_g) in electron volt (eV) computed at the PBE0//B3LYP/6-31G* level

Complexes	HOMO	LUMO	LUMO + 1	E_g	Exp[a]
Alq3	−5.26	−1.65	−1.40	3.86	2.81
3FAlq3	−5.52	−1.97	−1.73	3.79	–
4FAlq3	−5.49	−1.72	−1.49	4.00	–
5FAlq3	−5.35	−1.90	−1.66	3.69	2.66
6FAlq3	−5.63	−1.90	−1.65	3.98	2.93
7FAlq3	−5.37	−1.83	−1.58	3.79	2.81

[a] Experimental gap energies from [21]

Table 3 The HOMO, LUMO, and gap energies (E_g) in electron volt (eV) computed at the TD-PBE0//CIS/6-31G* level

Complexes	HOMO	LUMO	E_g
Alq3	−4.87	−1.65	3.22
3FAlq3	−5.12	−1.99	3.13
4FAlq3	−5.10	−1.67	3.43
5FAlq3	−4.84	−1.89	2.95
6FAlq3	−5.22	−1.89	3.33
7FAlq3	−4.92	−1.78	3.14

3.3 Photophysical properties

The absorption (λ_a) and emission (λ_e) wavelengths of *mer*-Alq3 have been computed by DFT theory, i.e., at the TD-B3LYP/6-31G* ($\lambda_a = 429$ nm and $\lambda_e = 533$ nm), TD-B3LYP/6-31+G* ($\lambda_a = 436$ nm and $\lambda_e = 543$ nm) [30], and TD-B3LYP/3-21 + G** ($\lambda_a = 415$ nm and $\lambda_e = 538$ nm) level [34]. In this study, we computed λ_a (410 nm) and λ_e (523 nm) of *mer*-Alq3 at the PBE0/6-31G* level which are in better agreement with experimental results [21]. So, we applied PBE0/6-31G* level for further study. In Table 4, we summarized the calculated and experimental [21] absorption and emission results.

Experimentally, the tendency in the absorption wavelengths is in the sequence of 5FAlq3 > 7FAlq3 > 6FAlq3. In our calculated results the trend has been found in the sequence of 5FAlq3 > 3FAlq3 ~ 7FAlq3 > *mer*-Alq3 > 6FAlq3 > 4FAlq3. The 3FAlq3, 5FAlq3, and 7FAlq3 are showing red shifts for the absorption spectra of ca. 12, 26, and 7 nm, respectively. The 4FAlq3 and 6FAlq3 are showing blue shifts for the absorption spectra of ca. 23 and 16 nm, respectively. In comparison with *mer*-Alq3, the emission spectra of 3FAlq3, 5FAlq3, and 7FAlq3 are red shifted ca. 24, 71, and 18 nm, respectively, while 4FAlq3 and 6FAlq3 are blue shifted ca. 51 and 26 nm, respectively. Generally, these results reflect the trends of the gap energy differences discussed in Sect. 3.2. From Table 4, it can be seen that in *mer*-Alq3 and its mono-fluorinated derivatives, the assignments for absorption are from HOMO to LUMO+1 while for emission are from LUMO to HOMO. It can be noted that for 5FAlq3 and 7FAlq3 where F is

Table 4 Calculated absorption (λ_a) and emission (λ_e) wavelengths of *mer*-Alq3 and its fluorinated derivatives in S_0 and S_1 states at the TD-PBE0/6-31G* level

Complexes	f[a]	Assignments[b]	S_0	Exp[c] (λ_a)	f[a]	Assignments[d]	S_1	Exp[c] (λ_e)
Alq3	0.0759	H → L + 1	410	387	0.0441	H ← L	523	515
3FAlq3	0.0684	H → L + 1	422	–	0.0411	H ← L	547	–
4FAlq3	0.0921	H → L + 1	387	–	0.0573	H ← L	472	–
5FAlq3	0.0668	H → L + 1	436	407	0.0365	H ← L	594	547
6FAlq3	0.0764	H → L + 1	394	375	0.0458	H ← L	497	495
7FAlq3	0.0766	H → L + 1	417	388	0.0427	H ← L	541	515

[a] f is oscillator strength

[b] H → L + 1 stands for HOMO to LUMO + 1

[c] Experimental λ_a and λ_e from [21]

[d] H ← L stands for LUMO to HOMO

taking part in the formation of HOMOs (see Figs. S1, S2), TD-PBE0 overestimates the absorption and emission wavelengths. Then we have calculated the absorption spectra at B3LYP, BLYP, SVWN, and B3PW91 functionals (see detail in Table S1), but all the functionals overestimate the wavelength results. Among all functionals PBE0 gives the best results. To check the basis set effect we also calculated the absorption spectra of 5FAlq3 at 6-31+G* and 3-21+G** basis sets by using PBE0; we found that basis set has no significant effect for the calculation of λ_a with the variation less than 5 nm. The 5FAlq3 and 7FAlq3 overestimate may be due to the F as it is taking part in the formation of HOMOs (for detail consult supporting information).

3.4 Energy partitioning analysis (EDA)

The EDA results of the mono-substituted fluorinated derivatives of *mer*-Alq3 are given in Table 5, where the ΔE_{elstat} % and ΔE_{orb} % denotes percentage contribution to the total attractive interaction, respectively [44, 45]. The electrostatic energies (ΔE_{elstat}) of 3FAlq3, 4FAlq3, 5FAlq3, 6FAlq3, and 7FAlq3 are 61.95, 62.10, 62.04, 62.15 and 61.88%, while orbital interaction energies (ΔE_{orb}) are 38.05, 37.90, 37.96, 37.85, and 38.12%, respectively. These results show that the electrostatic character is larger than covalent character which shows the similar trend with our previously reported work for *mer*-Alq3 [30] and nitrogen substituted derivatives of *mer*-Alq3 [33].

In Table 5, it can be found that the trend of ΔE_{elst} is L_a-AlL_bL_c > L_b-AlL_aL_c > L_c-AlL_aL_b, while ΔE_{oi} is L_b-AlL_aL_c > L_a-AlL_bL_c > L_c-AlL_aL_b in fluorinated derivatives of *mer*-Alq3. In fluorinated derivatives of *mer*-Alq3, the HOMOs are localized on A-ligand due to the weaker ΔE_{elst} between L_a-AlL_bL_c fragments, while LUMOs are localized on B-ligand due to the weaker ΔE_{oi} between L_b-AlL_aL_c fragments which show the similar trend to previously reported work for *mer*-Alq3 [30] and nitrogen substituted derivatives of *mer*-Alq3 [33].

3.5 Reorganization energy

The charge transfer rate can be described by Marcus theory via the following equation:

$$W = V^2 \Big/ h(\pi/\lambda k_B T)^{1/2} \exp(-\lambda/4k_B T) \quad (3)$$

There are two major parameters that determine self-exchange electron-transfer rates and ultimately charge mobility: (1) the electronic coupling V (transfer integral) between adjacent molecules, which needs to be maximized and (2) the reorganization energy λ, which needs to be small for significant transport. The λ contains the internal reorganization energy (λ_i) and the external polarization (λ_e). The λ_i reflects the change in molecular geometry associated with going from the neutral to the ionized state, or vice versa. The λ_e describes the change in electronic polarization of the surrounding molecules. This value is difficult to evaluate theoretically and consists of one of the challenges for theoretical chemists [46].

The internal reorganization energy (λ_i) is further divided into two parts: λ_i^1 and λ_i^2, where λ_i^1 corresponds to the geometry relaxation energy of one molecule from neutral state to charged state, and λ_i^2 corresponds to the geometry relaxation energy from charged state to neutral one [47, 48].

$$\lambda_i = \lambda_i^1 + \lambda_i^2 \quad (4)$$

In the evaluation of λ_i, the two terms were computed directly from the adiabatic potential energy surfaces [49, 50].

$$\begin{aligned}\lambda_i &= \lambda_i^1 + \lambda_i^2 \\ &= \left[E^{(1)}(X^+) - E^{(0)}(X^+)\right] + \left[E^{(1)}(X) - E^{(0)}(X)\right]\end{aligned} \quad (5)$$

Here, $E^{(0)}(X)$, $E^{(0)}(X^+)$ are the ground-state energies of the neutral and charged states, $E^{(1)}(X)$ is the energy of the

Table 5 Energy partitioning analysis of fluorinated derivatives of *mer*-Alq3 in ground state at the B3LYP/DZP level, using fragments L_i^- and $AlL_jL_k^+$ (all values in kcal/mol)

Complexes	Fragments	Energy components					
		ΔE_{int}	ΔE_{pauli}	ΔE_{elst}	ΔE_{oi}	ΔE_{elst} (%)	ΔE_{oi} (%)
3FAlq3	L_a-AlL_bL_c	−200.31	141.23	−210.16	−131.38	61.53	38.47
	L_b-AlL_aL_c	−201.63	145.95	−216.54	−131.05	62.30	37.70
	L_c-AlL_aL_b	−204.08	147.81	−218.22	−133.67	62.01	37.99
4FAlq3	L_a-AlL_bL_c	−200.16	141.27	−210.18	−131.25	61.56	38.44
	L_b-AlL_aL_c	−201.33	145.86	−217.25	−129.94	62.57	37.43
	L_c-AlL_aL_b	−203.93	147.19	−218.33	−132.79	62.18	37.82
5FAlq3	L_a-AlL_bL_c	−200.23	143.71	−211.66	−132.28	61.54	38.46
	L_b-AlL_aL_c	−201.28	147.37	−217.79	−130.87	62.46	37.54
	L_c-AlL_aL_b	−203.73	149.46	−219.38	−133.80	62.12	37.88
6FAlq3	L_a-AlL_bL_c	−200.86	139.42	−209.65	−130.64	61.61	38.39
	L_b-AlL_aL_c	−201.45	144.04	−216.32	−129.16	62.61	37.38
	L_c-AlL_aL_b	−204.20	145.16	−217.41	−131.96	62.23	37.77
7FAlq3	L_a-AlL_bL_c	−199.15	141.94	−208.99	−132.10	61.27	38.73
	L_b-AlL_aL_c	−199.87	146.90	−216.42	−130.35	62.41	37.59
	L_c-AlL_aL_b	−203.23	148.38	−217.90	−133.71	61.97	38.03

If Li^- is one of the three ligands, then $AlLjLk^+$ will be Al along with the two others

neutral molecule at the optimized charged geometry and $E^{(1)}(X^+)$ the energy of the charged state at the geometry of the optimized neutral molecule.

Lin et al. [51] calculated the reorganization energy of *mer*-Alq3 (reorganization energy for hole λ_i (h) = 0.242 eV and reorganization energy for electron λ_i (e) = 0.276 eV) at the B3LYP/6-31G* level. To compare the results of reorganization energy of fluorinated derivatives of *mer*-Alq3, we also calculated the reorganization energies of fluorinated derivatives of *mer*-Alq3 at the same level of theory. As shown in Table 6 λ_i (h) for 3FAlq3 is 0.233 eV which is almost the same as λ_i (h) of parent molecule, while λ_i (e) for 3FAlq3 is higher than that of *mer*-Alq3. The reorganization energies of 4FAlq3 to 7FAlq3 are higher than that of *mer*-Alq3 both for hole and electron. To calculate the transfer integral, crystal data are required which are not available; so we just calculated one of the important parameters of mobility, i.e., reorganization energy. It can be found that the mono-substitution of fluorine atom has no enhancing effect on the intrinsic charge mobility as compared to *mer*-Alq3.

Table 6 Calculated reorganization energies of *mer*-Alq3 and its fluorinated derivatives (in eV) for hole λ_i (h) and electron λ_i (e) at the B3LYP/6-31G* level

Complexes	λ_i (h)	λ_i (e)
Alq3[a]	0.242	0.276
3FAlq3	0.233	0.321
4FAlq3	0.246	0.296
5FAlq3	0.291	0.302
6FAlq3	0.306	0.307
7FAlq3	0.327	0.307

[a] Reorganization energies of Alq3 from [51]

4 Conclusions

A significant blue shift was predicted for 4-substituted 8-hydroxyquinoline derivative while red shift was observed for 5-substituted one, compared with *mer*-Alq3. The calculated absorption and emission wavelengths are in good agreement with available experimental data. The HOMOs are localized on A-ligand due to the weaker ΔE_{elst} between L_a-AlL_bL_c fragments, while the LUMOs are localized on B-ligand because L_b-AlL_aL_c fragments have weaker ΔE_{oi}. The mono-substitution of fluorine atom has no enhancing effect on the intrinsic charge mobility as compared to *mer*-Alq3.

Acknowledgments Financial supports from the NSFC (No. 50873032; 20773022), NCET-06-0321, JLSDP (20082212), and NENU-STB07007 are gratefully acknowledged. A. Irfan acknowledges the financial support from Ministry of Education, Pakistan.

References

1. Yeh SJ, Chen HY, Wu MF, Chan LH, Chiang CL, Yeh HC, Chen CT, Lee JH (2006) Org Electron 7:137. doi:10.1016/j.orgel.2005.12.004

2. Choi JH, Kim KH, Choi SJ, Lee HH (2006) Nanotechnology 17:2246
3. Sun Y, Giebink NC, Kanno H, Ma B, Thompson ME, Forrest SR (2006) Nature 440:908. doi:10.1038/nature04645
4. Williams EL, Haavisto K, Li J, Jabbour GE (2007) Adv Mater 19:197. doi:10.1002/adma.200602174
5. Chen CH, Shi J (1998) Coord Chem Rev 171:161
6. Curioni A, Boero M, Andreoni W (1998) Chem Phys Lett 294:263. doi:10.1016/S0009-2614(98)00829-X
7. Sugimoto M, Sakaki S, Sakanoue K, Newton MD (2001) J Appl Phys 90:6092. doi:10.1063/1.1415059
8. Han YK, Lee SU (2002) Chem Phys Lett 366:9. doi:10.1016/S0009-2614(02)01460-4
9. Fantacci S, Angelis FD, Sellon A (2003) J Am Chem Soc 125:4381. doi:10.1021/ja0207910
10. Amati M, Lelj F (2003) J Phys Chem A 107:2560. doi:10.1021/jp026981e
11. Lee T, Lin MS (2007) Cryst Growth Des 7:1803. doi:10.1021/cg070226e
12. Dice GD, Brett MJ, Wang D, Buriak JM (2007) Appl Phys Lett 90:253101. doi:10.1063/1.2749418
13. Tang CW, VanSlyke SA, Chen CH (1989) J Appl Phys 65:3610. doi:10.1063/1.343409
14. Yu J, Shen Z, Sakuratani Y, Suzuki H, Tokita M, Miyata S (1999) Jpn J Appl Phys 38:6762. doi:10.1143/JJAP.38.6762
15. Sapochak LS, Padmaperuma A, Washton N, Endrino F, Schmett GT, Marshall J, Fogarty D, Burrows PE, Forrest SR (2001) J Am Chem Soc 123:6300. doi:10.1021/ja010120m
16. Anderson S, Weaver MS, Hudson AJ (2000) Synth Met 111:459. doi:10.1016/S0379-6779(99)00400-2
17. Jang H, Do LM, Kim Y, Kim JG, Zyung T, Do Y (2001) Synth Met 121:1669
18. Burrows PE, Shen Z, Bulovic V, McCarty DM, Forrest SR, Cronin JA, Thompson ME (1996) J Appl Phys 79:7991. doi:10.1063/1.362350
19. Hopkins TA, Meerholz K, Shaheen S, Anderson ML, Schmidt A, Kippelen B, Padias AB, Hall HK Jr, Peyghambarian N, Armstrong NR (1996) Chem Mater 8:344. doi:10.1021/cm9503442
20. Maienfisch P, Hall RG (2004) Chimia. Inter J Chem 58:93
21. Shi YW, Shi MM, Huang JC, Chen HZ, Wang M, Liu XD, Ma YG, Xu H, Yang B (2006) Chem Commun 18:1941. doi:10.1039/b516757d
22. te Velde G, Bickelhaupt FM, Baerends EJ, Fonseca Guerra C, van Gisbergen SJA, Snijders JG, Ziegler T (2001) J Comput Chem 22:931. doi:10.1002/jcc.1056
23. Lee VY, Kato R, Sekiguchi A, Krapp A, Frenking G (2007) J Am Chem Soc 129:10340. doi:10.1021/ja0740162
24. Krapp A, Pandey KK, Frenking G (2007) J Am Chem Soc 129:7596. doi:10.1021/ja0691324
25. Bessac F, Frenking G (2003) Inorg Chem 42:7990. doi:10.1021/ic034141o
26. Bickelhaupt FM, Baerends EJ (2000) Kohn–Sham density functional theory: predicting and understanding chemistry. In: Lipkowitz KB, Boyd DB (eds) Rev Comput Chem, vol 15. Wiley-VCH, New York, pp 1–86
27. Ziegler T, Rauk A (1977) Theor Chim Acta 46:1
28. Morokuma K (1971) J Chem Phys 55:1236. doi:10.1063/1.1676210
29. Frisch MJ et al (2004) Gaussian 03, revision B.03, Gaussian, Wallingford
30. Zhang J, Frenking G (2004) J Phys Chem A 108:10296. doi:10.1021/jp0489774
31. Zhang J, Frenking G (2004) Chem Phys Lett 394:120. doi:10.1016/j.cplett.2004.06.074
32. Gahungu G, Zhang J (2005) J Phys Chem B 109:17762. doi:10.1021/jp052220a
33. Irfan A, Cui R, Zhang J (2008) J Mol Struct THEOCHEM 850:79. doi:10.1016/j.theochem.2007.10.029
34. Halls MD, Schlegel HB (2001) Chem Mater 13:2632. doi:10.1021/cm010121d
35. Gahungu G, Zhang J (2005) Chem Phys Lett 410:302. doi:10.1016/j.cplett.2005.05.086
36. Yang Z, Yang S, Zhang J (2007) J Phys Chem A 111:6354. doi:10.1021/jp068589x
37. Hu B, Gahungu G, Zhang J (2007) J Phys Chem A 111:4965. doi:10.1021/jp0689215
38. Sun M, Niu B, Zhang J (2008) J Mol Struct THEOCHEM 862:85. doi:10.1016/j.theochem.2008.04.038
39. Adamo C, Barone V (1999) J Chem Phys 110:6158. doi:10.1063/1.478522
40. Petersson GA, Bennett A, Tensfeldt TG, Al-Laham MA, Shirley WA, Mantzaris J (1988) J Chem Phys 89:2193. doi:10.1063/1.455064
41. ADF 2006.01, SCM, Theoretical chemistry, Vrije Universiteit, Amsterdam
42. van Lenthe E, Ehlers A, Baerends EJ (1999) J Chem Phys 110:8943. doi:10.1063/1.478813
43. Brinkmann M, Gadret G, Muccini M, Taliani C, Masciocchi N, Sironi A (2000) J Am Chem Soc 122:5147. doi:10.1021/ja993608k
44. Frunzke J, Lein M, Frenking G (2002) Organometallics 21:3351
45. Esterhuysen C, Frenking G (2004) Theor Chem Acc 111:381. doi:10.1007/s00214-003-0535-2
46. Soos ZG, Tsiper EV, Painelli A (2004) J Lumin 110:332. doi:10.1016/j.jlumin.2004.08.029
47. Gruhn NE, da Silva Filho DA, Bill TG, Malagoli M, Coropceanu V, Kahn A, Brédas JL (2002) J Am Chem Soc 124:7918. doi:10.1021/ja0175892
48. Reimers JR (2001) J Chem Phys 115:9103. doi:10.1063/1.1412875
49. Brédas JL, Beljonne D, Coropceanu V, Cornil J (2004) Chem Rev 104:4971. doi:10.1021/cr040084k
50. Coropceanu V, Nakano T, Gruhn NE, Kwon O, Yade T, Katsukawa K, Brédas JL (2006) J Phys Chem B 110:9482. doi:10.1021/jp060855j
51. Lin BC, Cheng CP, You ZQ, Hsu CP (2005) J Am Chem Soc 127:66. doi:10.1021/ja045087t